8(2011) 429 – 443

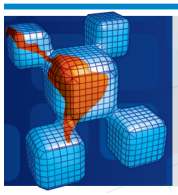

Latin American Journal of Solids and Structures
www.lajss.org

# On the effect of the near field records on the steel braced frames equipped with energy dissipating devices

**Abstract**

The behavior of braced steel frame structures is of special importance due to its extensive use. Also the application of active and semi-active control systems, regarding to their benefits in obtaining better seismic performance has increased significantly. The majority of the works on steel structures and steel connections has been done under far field records, and the behavior of steel frame structures equipped with yielding dampers under these circumstances has not yet been fully analyzed. The main purpose of this paper is to determine the behavior of structures equipped with yielding dampers, located in near field based on energy concepts. In order to optimize their seismic behavior, the codes and solutions are also presented.The selected system is a braced steel frame system which is equipped with yielding dampers and the analysis is performed using the "Perform 3D V.4" software and the conclusions are drawn upon energy criterion. The effect of PGA variation and height of the frames are also considered in the study .Finally, using the above mentioned results, a proper solution is presented for typical systems in order to increase the energy damping ability and reduce the destructive effects in structures on an earthquake event, so that a great amount of induced energy is damped and destruction of the structure is prevented as much as possible.

**Keywords**

yielding dampers (ADAS), steel braced frame, energy dissipation devices, near-fault records.

**Mahmoud Bayat**[a,*] **and Gholamreza Abdollahzadeh**[b]

[a] Department of Civil Engineering, Shomal University, Amol, Iran [b] Department of Civil Engineering, Babol University of Technology, Babol, Iran

Received 23 Mar 2011;
In revised form 17 Oct 2011

* Author email: mbayat14@yahoo.com

## 1 INTRODUCTION

Analyzing nonlinear dynamic model of structures is an interesting area in nonlinear science. During the past few decades, many authors consider the dynamic modeling with damping and without damping and try to analysis them analytically and numerically [1–8, 14, 20, 23, 25].

The ideas of using metallic energy dissipaters in earthquake design have been considered a lot in the previous studying. Kelly et al [17] developed the work on the Mechanisms of energy absorption in special devices for use in earthquake resistant structures. Skinner et

all [24] considered the Hysteretic dampers for earthquake-resistant structures. Kelly et al [16] had a concentrate review on current uses of energy absorbing devices. To dissipate the energy present in the vibration of a structure during an earthquake, the inelastic deformation of metals can be effective. Many researchers have been worked based on the use of low-yield metals with triangular and hourglass shapes. Among the best known devices are the patented added damping and stiffness device (ADAS) and variations such as the TADAS. These devices exhibit stable hysteretic behavior; they are insensitive to thermal effects, and extremely reliable. A typical $X$-shaped plate damper or ADAS (added damping and stiffness) device is shown in Fig. 1. Bergaman et al [9] evaluated the cyclic testing of steel-plate devices for added damping and stiffness. Whittaker et al [35] worked on the Seismic testing of steel plate energy dissipation devices. Tsai et al [32] studied on the Design of steel triangular plate energy absorbers for seismic-resistant construction. Kobori et al [18] developed the work on the application of hysteresis steel dampers. ADAS devices have been used in the seismic retrofit of several structures in Mexico City [28]. Two important aspects in the use of energy dissipating devices in earthquake engineering applications are: (i) to have a stable and sufficiently large dissipation capacity capable of controlling the earthquake response of the structure, and (ii) to have a representative model of its cyclic behavior. Plasticity in low-yield metals satisfies the first condition as long as geometric effects due to large deformations in the device are not significant. On the other hand, several models of increasing accuracy have been proposed to represent the cyclic behavior of steel dampers subject to small deformations [12, 27, 31, 35]. The role of a passive energy dissipator is to increase the hysteretic damping in the structure. This study mainly focuses on the effects of application of ADAS devices – discussing the basic concepts of energy under the near field records. To show the effects and performance of ADAS devices when severe earthquakes occur, three cases consist of five, ten and fifteen–story 3-bay Concentric Braced Frames equipped with and without ADAS devices have been considered. The assumed detail and arrangement of typical ADAS devices are shown in Figure 1.

Many near-fault ground motions have resulted in serious fatalities and severe damage to buildings and bridges in the vicinity of seismic sources during some infamous earthquakes, such as the 1994 Northridge (USA), 1995 Kobe (Japan), 1999 Chi-Chi (Taiwan) earthquakes [11, 15, 19]. Near-fault earthquakes usually have the following features:

1. A high level of peak ground acceleration,
2. A large vertical ground motion,
3. An intense long-period velocity pulse wave.

For the third feature, the velocity pulse that usually occurs at the beginning of a near-fault earthquake is also referred to as the forward rupture directivity effect [10, 29].

Baker [32] proposed an equation and according to that, the pulse period usually can range from 1.4 s to 7 s for a range of earthquake magnitudes from 6 to 7.6 M.

In order to improve the performance and safety of near-fault seismic structures, some researchers have proposed using semi-active isolation systems (also referred to as smart isolation

systems) [26, 30]. Bayat considered the work on the steel braced frame structures equipped with ADAS devices under the far field record and in this study, which is an extension of the authors' previous works [1], the effect of the near field records is considered on the steel braced frames equipped with energy dissipating devices. The near-fault earthquake characteristics outlined above should be considered in the design of structures located in near-fault regions.

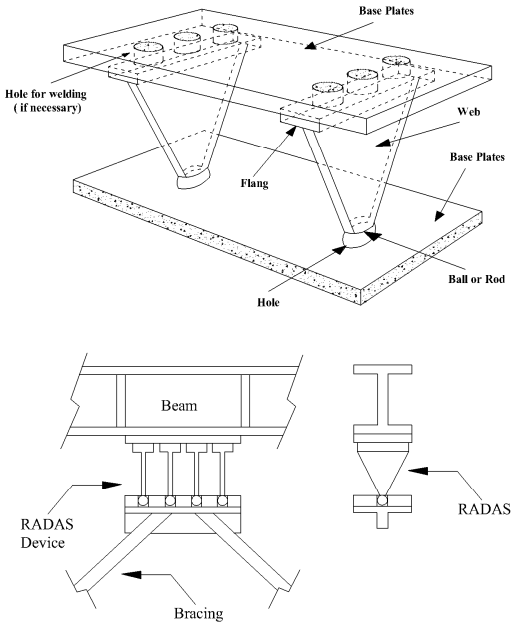


Figure 1 Arrangement of ADAS devices [1, 21].

## 2 OVER REVIEW OF INPUT ENERGY TO A STRUCTURE

Mathematical formulation of a viscous damped SDOF system subject to horizontal earthquake ground motion is [1];

$$m\ddot{u}_t + c\dot{u} + f_s = 0 \tag{1}$$

If we choose $\ddot{u}_t = \ddot{u} + \ddot{u}_g$ = absolute (total) displacement of mass, the equation (1) can be written as ;

$$m\ddot{u} + c\dot{u} + f_s = -m\ddot{u}_g \tag{2}$$

In which ;
$u$ = relative displacement of the mass with respect to the ground,
$u_g$ = earthquake ground displacement.
Integrate Eq. (2) with respect to $u$:

$$\int m\ddot{u}\,du + \int c\dot{u}\,du + \int f_s du = -\int m\ddot{u}_g\,du \tag{3}$$

We achieve these kinds of energies [1];

$$E_I = E_k + E_D + E_A \tag{4}$$

$E_I$ = Input energy
$E_k$ = Kinetic energy;
$E_D$ = Damping energy
$E_A = \int f_s du = E_s + E_H$ = Composed of recoverable elastic strain energy and irrecoverable hysteretic energy.

The Equation (4) is the "Relative" Energy Equation [1, 33].

In this study we considered the "relative" energy method for evaluation of input energy of structures and the total input energy of structures are compared at the time when the earthquake is over and the motion of structure is damped.

For a fixed $E_I$, it is better to increase the $E_H$ then the elastic strain energy in the structure becomes minimized.

## 3 DESIGNING OF ADAS DEVICES

The ADAS devices bearable forces are given as [1, 21];

$$F_R = K'\delta_y + aK'(\delta_R - \delta_y), \tag{5}$$

$a$ = an unknown coefficient to be determined from the experimental data
$K'$= elastic stiffness of the ADAS devices
$\delta_R$ = maximum relative displacement
$\delta_y$ = yield displacement of the ADAS devices

## 4 CHARACTERISTICS OF THE NEAR FIELD EARTHQUAKE RECORDS

Table 1 is the details of the unscaled earthquake records. In this study, scaled records are used for nonlinear dynamic analysis with PGA scaled to 0.4g, 0.6g and 0.8g. Figure 2a-c represent the acceleration recorded during three earthquake near field records (Tabas, Northridge and Imperial Valley) with PGA = 0.4g.

## 5 NONLINEAR DYNAMIC TIME HISTORY ASSUMPTIONS

In this study we considered the same structures with dampers and without any dampers have been analyzed to show the great effect of these energy dissipating devices. The ADAS devices lower 80 percent of the column shear forces using this procedure when the whole system is subjected to different Earthquake ground movements. Nonlinear time history analysis involves the

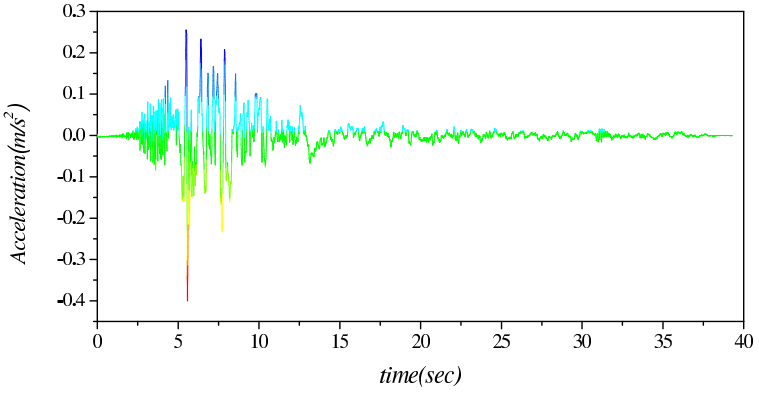


(a) Tabas

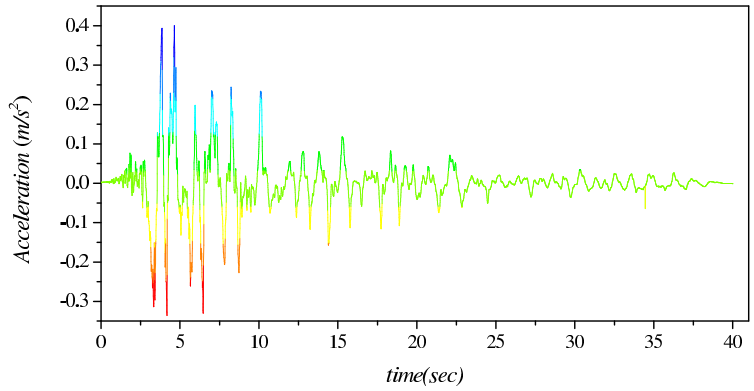


(b) Northridge

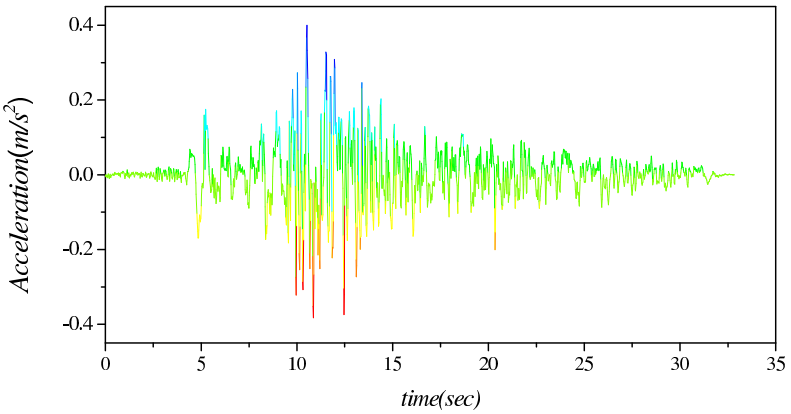


(c) Imperial Valley

Figure 2 Acceleration recorded during the near field earthquakes (PGA = 0.4g).

Table 1 Unsealed earthquake records used for non-linear analysis.

| | Near field | | |
|---|---|---|---|
| Earthquake | Imperial Valley 1979/10/15 | Northridge 1994/01/17 | Tabas,Iran 1978/09/16 |
| Magnitude | M(6.5)Ml(6.6) Ms(6.9) | M(6.7)Ml(6.6) Ms(6.7) | M(7.4)Ml(7.7) Ms(7.4) |
| Station | 952 El Centro | 74 Sylmar-Converter Sta | 9101 Tabas |
| Data source | USGS | DWP | ——— |
| PGA | 0.519 | 0.612 | 0.836 |
| Distance(Km) | Closest to fault rapture (1.0) | Closest to fault rapture (6.2) | Hypocentral (3.0) |
| Site Condition | CWB(D) USGS(C) | CWB(C) USGS(C) | CWB(C) |

computation of dynamic response at each time increment concerning due consideration given to the inelasticity in members. Hysteretic energy under cyclic loading is evaluated and tabulated. During strong and mediocre earthquakes, structures enter the plastic range. Therefore, it is essential to perform a nonlinear analysis. For this purpose, numerical simulations were carried out by PERFORM 3D.V4 [34].

The frames were designed prior to this study in accordance with Uniform Building Code 97 requirements, based upon the static analysis.

We consider following criterias for this study;

1. Soil type is assumed Sc (very dense soil and soft rock) according to UBC97 [22] code.
2. Earthquake source and structures distance from active fault is 10 km according to type A of UBC97.
3. It is assumed that structures are located in zone 4, according to UBC97.
4. The P-Delta effect is included in the analysis.
5. The non-linear behavior of models is assumed from FEMA273 [13]
6. The plastic hinges in analysis are assumed perfectly elastic-plastic.
7. A 0.005s time step be used for all non-linear analysis of models.
8. Strength loss is ignored in non-linear analysis of systems.
9. The value of $a$ in Eq.(5) = 0.12

10. Poisson's ratio = 0.3

11. Elastic modulus = 2.0 $\times 10^6$ kPa

12. Yield stress = 2400 $\frac{Kg}{cm^2}$

13. The properties of dampers are shown in Table 2.

14. Most of the inelastic components in PERFORM-3D have the same form for the F-D relationship. Figure 3 shows a trilinear relationship with optional strength loss.

Table 2 The properties of dampers.

| Type of the damper | The Geometric properties | | | | | | |
|---|---|---|---|---|---|---|---|
| | h (cm) | b-top & bottom (cm) | B middle (cm) | t (cm) | $\Delta y$ (cm) | $Py$ (Kg) | $K$ (Kg/cm) |
| AADAS | 12.7 | 6.35 | 1.27 | 0.64 | 0.2794 | 306 | 1094 |

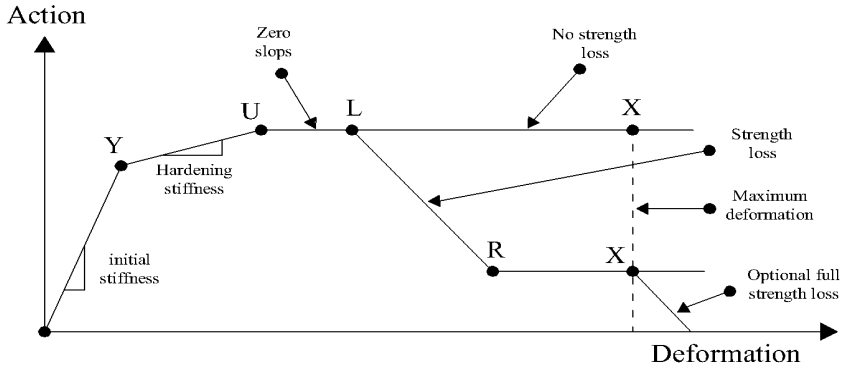


Figure 3 PERFORM Action-Deformation Relationship [22].

The key points in the relationship are as follows;

1. **Y Point.** This is the first yield point, where significant nonlinear behavior begins [34].

2. **U Point.** This is the ultimate strength point, where the maximum strength is reached [34].

3. **L Point.** This is the ductile limit point, where significant strength loss begins [34].

4. **R Point.** This is the residual strength point, where the minimum residual strength is reached [34].

5. **X Point.** This is usually at a deformation that is so large that there is no point in continuing the analysis. You can continue an analysis beyond this point if you wish, but usually you will stop the analysis if any component is deformed beyond its X point [34].

Figure 4 shows a type single CBF and ADAS farmes which are considered in this study.

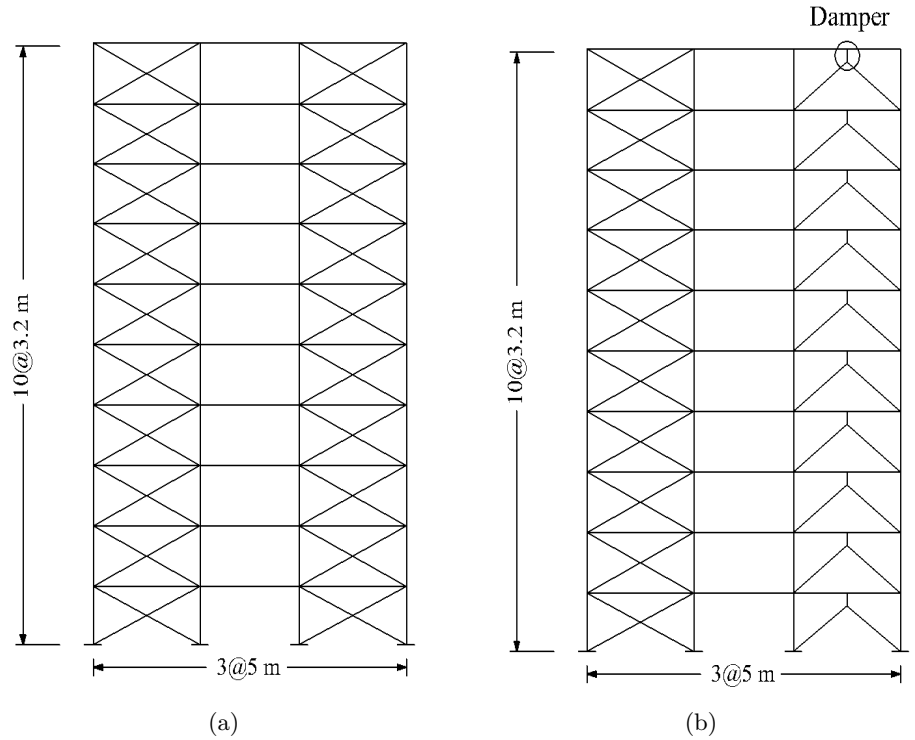


Figure 4 Type of studied single frame (a) , b) ADAS.

## 6 RESULTS AND DISCUSSIONS

### 6.1 Input energy

It is obvious that the input energy to a structure is a function of time. In this paper we evaluated the total input energy in the structure to compare their behavior. Table 3 represents the maximum total input energy in different systems.

### 6.2 Hysteretic energy

The maximum total hysteretic energy at the end of the earthquake is used for comparing in different structural systems. Table 4 shows the maximum total hysteretic energy in different systems.

To show the effectiveness of using ADAS devices in the following sections we consider the

Table 3 The maximum total input energy per mass (m/sec)$^2$ in different systems under different earthquakes.

| Earthquake | Number of Bay | PGA | 5 STORY | | 10 STORY | | 15 STORY | |
|---|---|---|---|---|---|---|---|---|
| | | | ADAS | CBF | ADAS | CBF | ADAS | CBF |
| Imperial Valley | 3 Bay | 0.4g | 0.145 | 0.076 | 0.216 | 0.078 | 0.304 | 0.158 |
| | | 0.6g | 0.338 | 0.183 | 0.466 | 0.179 | 0.620 | 0.336 |
| | | 0.8g | 0.619 | 0.332 | 0.829 | 0.358 | 1.067 | 0.593 |
| Northridge | 3 Bay | 0.4g | 0.419 | 0.681 | 1.003 | 0.580 | 1.463 | 0.690 |
| | | 0.6g | 1.192 | 1.415 | 2.399 | 1.471 | 3.215 | 1.631 |
| | | 0.8g | 2.755 | 2.349 | 4.491 | 2.732 | 5.711 | 2.842 |
| Tabas | 3 Bay | 0.4g | 0.323 | 0.183 | 0.566 | 0.185 | 0.566 | 0.185 |
| | | 0.6g | 0.786 | 0.451 | 1.256 | 0.441 | 1.256 | 0.441 |
| | | 0.8g | 1.485 | 0.881 | 2.209 | 0.832 | 2.209 | 0.832 |

Table 4 The maximum total hysteretic energy per mass (m/sec)$^2$ in different systems under different earthquakes.

| Earthquake | Number of Bay | PGA | 5 STORY | | 10 STORY | | 15 STORY | |
|---|---|---|---|---|---|---|---|---|
| | | | ADAS | CBF | ADAS | CBF | ADAS | CBF |
| Imperial Valley | 3 Bay | 0.4g | 0.077 | 0.008 | 0.068 | 0.000 | 0.095 | 0.019 |
| | | 0.6g | 0.168 | 0.050 | 0.139 | 0.028 | 0.217 | 0.135 |
| | | 0.8g | 0.272 | 0.124 | 0.225 | 0.121 | 0.369 | 0.332 |
| Northridge | 3 Bay | 0.4g | 0.129 | 0.009 | 0.133 | 0.011 | 0.151 | 0.048 |
| | | 0.6g | 0.290 | 0.087 | 0.266 | 0.075 | 0.358 | 0.190 |
| | | 0.8g | 0.486 | 0.270 | 0.420 | 0.219 | 0.633 | 0.414 |
| Tabas | 3 Bay | 0.4g | 0.168 | 0.009 | 0.185 | 0.021 | 0.191 | 0.072 |
| | | 0.6g | 0.383 | 0.115 | 0.367 | 0.114 | 0.462 | 0.226 |
| | | 0.8g | 0.652 | 0.388 | 0.572 | 0.294 | 0.834 | 0.455 |

ratio of the hysteretic energy to the input energy and the effect of different parameters like the height of structures, increasing and decreasing of the PGA's.

### 6.3 Effect of increase or decrease in structure height on the ratio of hysteretic energy to input

Figures 5a-c show the comparison of the (Eh/Ei) ratio under for the different near field earthquake records. Figure 6 represents the average diagram with respect to near field earthquake records and the type of systems. Fig. 6 Shows the effect of changes in the structure height on the input energy in the ADAS and CBF systems, under the near field records.

From Figs. 5a-c and Fig. 6 the input energy increases in the CBF system by increasing in height and decreases in ADAS systems by increasing in height especially in 10 story buildings. It is observe from Fig. 6 the performance of the ADAS systems is better in 5 story buildings under the near field records.

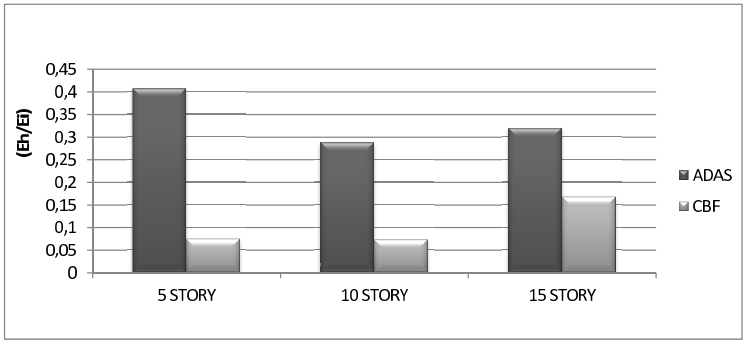


(a) Imperial Valley

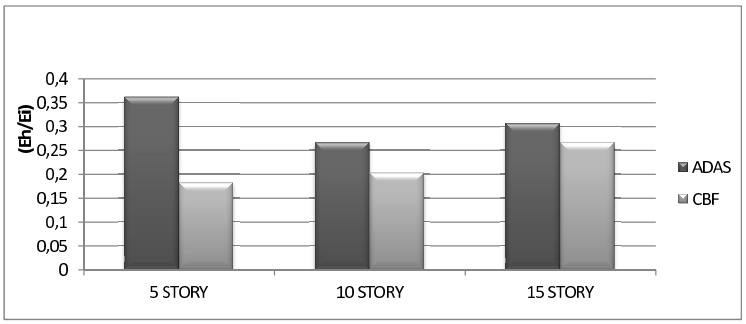


(b) Northridge

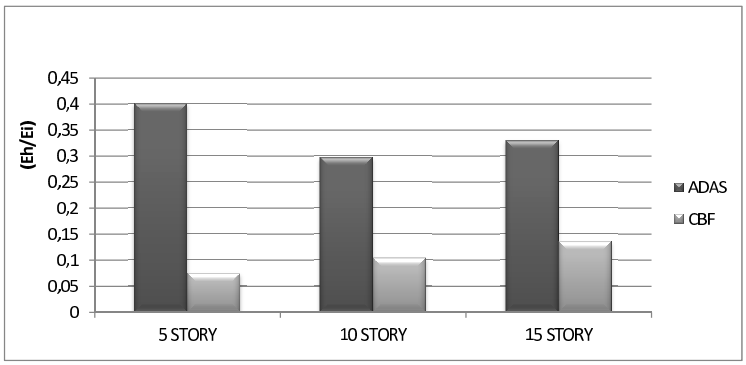


(c) Tabas

Figure 5 Comparison of the (Eh/Ei) ratio under near field records.

Table 5 The ratio of the hysteretic energy to the input energy in different systems under different earthquakes.

| Earthquake | Number of Bay | PGA | 5 STORY | | 10 STORY | | 15 STORY | |
|---|---|---|---|---|---|---|---|---|
| | | | ADAS | CBF | ADAS | CBF | ADAS | CBF |
| Imperial Valley | 3 Bay | 0.4g | 0.466 | 0.030 | 0.28 | 0.00 | 0.314 | 0.053 |
| | | 0.6g | 0.434 | 0.080 | 0.27 | 0.06 | 0.350 | 0.181 |
| | | 0.8g | 0.384 | 0.110 | 0.24 | 0.14 | 0.346 | 0.252 |
| Northridge | 3 Bay | 0.471 | 0.155 | 0.260 | 0.131 | 0.375 | 0.220 | 0.471 |
| | | 0.384 | 0.192 | 0.214 | 0.215 | 0.372 | 0.274 | 0.384 |
| | | 0.250 | 0.205 | 0.164 | 0.258 | 0.371 | 0.297 | 0.250 |
| Tabas | 3 Bay | 0.455 | 0.014 | 0.295 | 0.044 | 0.312 | 0.087 | 0.455 |
| | | 0.427 | 0.075 | 0.263 | 0.104 | 0.348 | 0.142 | 0.427 |
| | | 0.384 | 0.129 | 0.233 | 0.141 | 0.363 | 0.180 | 0.384 |

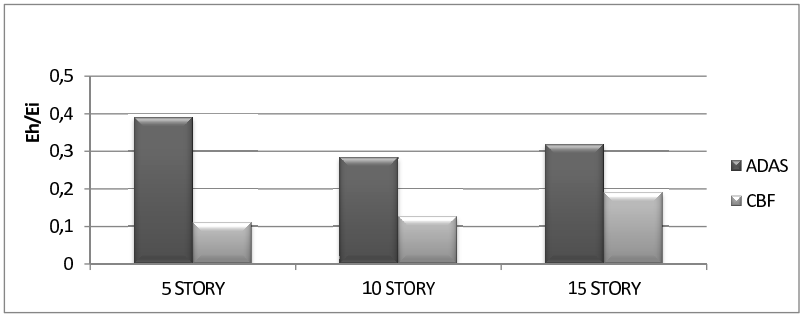


Figure 6 The effect of height of structure on (Eh/Ei) under near field records.

### 6.4 Effect of PGA variation on the ratio of the hysteretic energy to input energy

Figs. 7a-c show the effect of the maximum acceleration of the near field records with PGA 0.4g, 0.6g, 0.8g for 5, 10, 15 story buildings. As it is shown in the figures the value of the ratio (Eh/Ei) in the steel braced frame equipped with ADAS devices is more than the CBF systems. This value of the ratio increases with the PGA. The hysteretic-to-input ratio is almost constant for the ADAS system with increasing PGA which means nothing but limitation for an ADAS system in absorption of the hysteretic energy in high values of PGA; nonetheless, the value of hysteretic-to-input ratio is much higher in the ADAS system than that in a CBF one.

Fig. 8 is the average diagram from figures 7a to 7c under the near field records. As it is shown in the Fig. 8, the value of the hysteretic-to-input ratio decreases in ADAS systems with PGA increase and increases for CBF systems, increases with PGA increase. Generally, we can conclude that in the records of the near field, performance of the ADAS systems outstrips that of the CBF ones. Great amount of hysteretic energy were damped in the ADAS devices as it is obvious in the hysteretic-to-input ratio. The goal of using hysteretic dampers is to increase the hysteretic-to-input ratio in structures as it is indicated in this study.

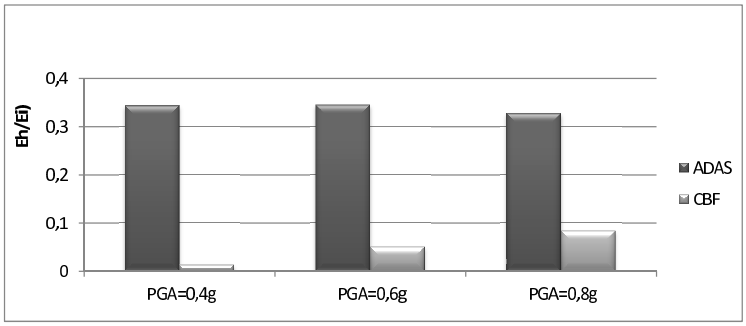


(a) Imperial Valley

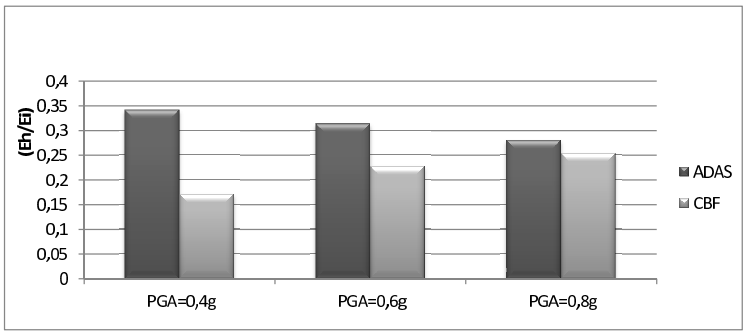


(b) Northridge

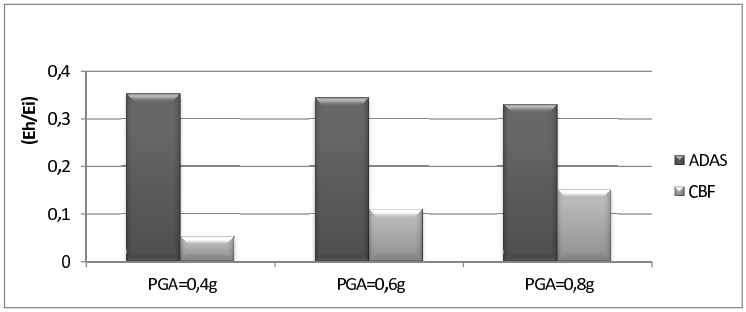


(c) Tabas

Figure 7 The relation between the ratio of the hysteretic energy to input energy with PGA under near field records.

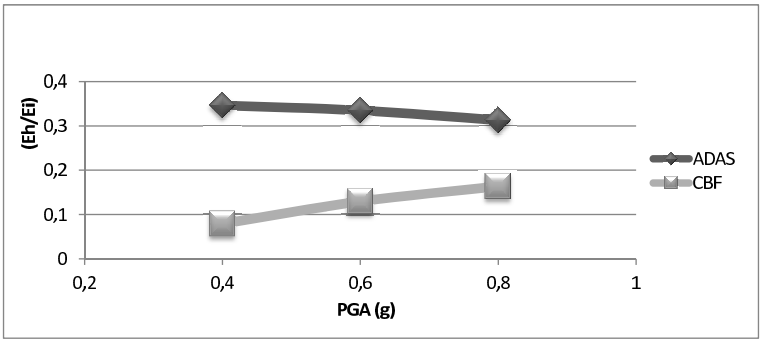


Figure 8 The relation between the ratio of the hysteretic energy to input energy with PGA under near field record.

## 7 CONCLUSION

In this study the effect of the near field records have considered on the steel braced frames with energy dissipating devices (ADAS) and without ADAS devices. Many near-fault ground motions have resulted in serious fatalities and severe damage to buildings and bridges in the vicinity of seismic sources during some infamous earthquakes. We have observed from the behavior of the structures located in the near filed region based upon the frequency content of the earthquake, depends on the geometric specifications of the building including its height. This study shows the difference of building behaviors with and without damper during earthquake vibrations under the near field records. The influences of the near field records have not too much impact on the 5 story and 10 story building in ADAS systems. In other words the performance of these structures in the near filed region is better than the other structural systems which were considered in this study. The ADAS devices significantly increase the resistance of the structure components to the dynamic loads and they are effective in reducing the seismic response of the structures. The benefits of the energy dissipaters have been clearly demonstrated by these comparative data and the improvement in performance of structures during earthquake excitation have been proved.

## References

[1] M. Bayat and G. R. Abdollahzadeh. Analysis of the steel braced frames equipped with adas devices under the far field records. *Latin American Journal of Solids and Structures*, 8(2):163–181, 2011.

[2] M. Bayat, A. Barari, and M. Shahidi. Dynamic response of axially loaded euler-bernoulli beams. *Mechanika*, 17(2):172–177, 2011.

[3] M. Bayat, M. Bayat, and M. Bayat. An analytical approach on a mass grounded by linear and nonlinear springs in series. *Int. J. Phy. Sci.*, 6(2):229–236, 2011.

[4] M. Bayat and I. Pakar. Application of He's energy balance method for nonlinear vibration of thin circular sector cylinder. *Int. J. Phy. Sci.*, 6(23):5564–5570, 2011.

[5] M. Bayat, I. Pakar, and M. Bayat. Analytical study on the vibration frequencies of tapered beams. *Latin American Journal of Solids and Structures*, 8(2):149–162, 2011.

[6] M. Bayat, M. Shahidi, A. Barari, and G. Domairry. The approximate analysis of nonlinear behavior of structure under harmonic loading. *Int.J. Phy. Sci.*, 5(7):1074–1080, 2010.

[7] M. Bayat, M. Shahidi, A. Barari, and G. Domairry. Analytical evaluation of the nonlinear vibration of coupled oscillator systems. *Zeitschrift fur Naturforschung Section A-A Journal of Physical Sciences*, 66(1-2):67–74, 2011.

[8] M. Bayat, M. Shahidi, and M. Bayat. Application of iteration perturbation method for nonlinear oscillators with discontinuities. *Int. J. Phy. Sci.*, 6(15):3608–3612, 2011.

[9] D.M. Bergaman and S.C. Goel. Evaluation of cyclic testing of steel-plate devices for added damping and stiffness. Technical Report UMCE 87-10, University of Michigan, Ann Arbor, Michigan, 1987.

[10] D.J. Bray and A. Rodriguez-Marek. Characterization of forward-directivity ground motions in the near-fault region. *Soil Dyn Earthq Eng*, 11:815–28, 2004.

[11] J.F. Chai and C.H. Loh. Near-fault ground motion and its effect on civil structures. In *International workshop on mitigation of seismic effects on transportation structures*, pages 70–81, 2000.

[12] G.F. Dargush and T.T. Soong. Behavior of metallic plate dampers in seismic passive energy dissipation systems. *Earthquake Spectra*, 11(4):545–568, 1995.

[13] FEMA 273, NEHRP guidelines and commentary for the seismic rehabilitation of buildings. Technical Report FEMA 273 (Guidelines), Federal Emergency Management Agency, Washington, D.C., 1997.

[14] E. Ghasemi, M. Bayat, and M. Bayat. Visco-elastic MHD flow of walters liquid b fluid and heat transfer over a non-isothermal stretching sheet. *Int. J. Phy. Sci.*, 6(21):5022–5039, 2011.

[15] J.F. Hall, T.H. Heaton, M.W. Halling, and D.J. Wald. Near-source ground motion and its effects on flexible buildings. *Earthq Spectra*, 11:569–605, 1995.

[16] J.M. Kelly and R.I. Skinner. A review of current uses of energy absorbing devices. Technical Report UCB=EERC-79=10, University of California, Berkeley, 1979.

[17] J.M. Kelly, R.I. Skinner, and A.J. Heine. Mechanisms of energy absorption in special devices for use in earthquake resistant structures. *Bulletin of the New Zealand Society for Earthquake Engineering*, 5:63–88, 1972.

[18] T. Kobori, Y. Miura, E. Fukusawa, T. Yamada, T. Arita, Y. Takenaka, N. Miyagawa, N. Tanaka, and T. Fukumoto. Development and application of hysteresis steel dampers. In *Proceedings of the 10th World Conference on Earthquake Engineering*, pages 2341–2346, 1992.

[19] C.H. Loh, T.C. Wu, and N.E. Huang. Application of the empirical mode decomposition-hilbert spectrum method to identify near-fault ground-motion characteristics. *Bull Seismol Soc Amer*, 91:1339–57, 2001.

[20] I. Pakar and M. Bayat. Analytical solution for strongly nonlinear oscillation systems using energy balance method. *Int. J. Phy. Sci.*, 6(22):51665170, 2011.

[21] W. Pong, Z. Lee, C.S. Tsai, and B.J. Chen. Heuristic design procedure for structures with displacement dependent damping devices. *Engineering Computations*, 26(4):347–359, 2009.

[22] RAM International, L.L.C., University of California. *PERFORM 3D.V4, analysis software.*

[23] M. Shahidi, M. Bayat, I. Pakar, and G. R. Abdollahzadeh. On the solution of free non-linear vibration of beams. *Int. J. Phy. Sci.*, 6(7):1628–1634, 2011.

[24] R.I. Skinner, J.M. Kelly, and A.J. Heine. Hysteretic dampers for earthquake-resistant structures. *Earthquake Engineering and Structural Dynamics*, 3:287–296, 1975.

[25] K.S. Soleimani, E. Ghasemi, and M. Bayat. Mesh-free modeling of two-dimensional heat conduction between eccentric circular cylinders. *Int. J. Phy. Sci.*, 6(16):4044–4052, 2011.

[26] B.F. Spencer, J.C. Ramallo, and E.A. Johnson. Smart base isolation systems. *J Eng Mech*, 128(10):1088–100, 2002.

[27] A. Tena-Colunga. Mathematical modelling of the adas energy dissipation device. *Engineering Structures*, 19(10):811–821, 1997.

[28] A. Tena-Colunga and A. Vergara. Seismic retrofit of a mid-rise building using steel bracing or ADAS energy dissipation devices: a comparative study. In *Proceedings of the 11th World Conference on Earthquake Engineering*, Mexico, DF, 1996.

[29] P. Tothong, C.A. Cornell, and J.W. Baker. Explicit directivity-pulse inclusion in probabilistic seismic hazard analysis. *Earthq Spectra*, 23(4):867–91, 2007.

[30] C.S. Tsai and H.H. Le. Applications of viscoelastic dampers to high-rise buildings. *J Struct Eng, ASCE*, 119(4):1222–33, 1993.

[31] C.S. Tsai and K.C. Tsai. TPEA device as a seismic damper for high-rise buildings. *Journal of Engineering Mechanics (ASCE)*, 121(10):1075–1081, 1995.

[32] K.C. Tsai, H.W. Chen, C.P. Hong, and Y.F. Su. Design of steel triangular plate energy absorbers for seismic-resistant construction. *Earthquake Spectra*, 9(3):505–528, 1993.

[33] C.-M. Uang and V.V. Bertero. Use of energy as a design criterion in earthquake resistant design. Technical Report UCB/EERC-88/18, Earthquake Eng. Res. Ctr, Univ. of California, Berkeley, 1988.

[34] *Uniform Building Code*, 1997.

[35] A.S. Whittaker, V.V. Bertero, C.L. Thompson, and L.J. Alonso. Seismic testing of steel plate energy dissipation devices. *Earthquake Spectra*, 7(4):563–604, 1991.